Electromagnetic field and eddy currents in the mantle of the ore-smelting furnace

IOP Conf. Series: Materials Science and Engineering **560** (2019) 012053 doi:10.1088/1757-899X/560/1/012053

Electromagnetic field and eddy currents in the mantle of the ore-smelting furnace

A V Blanc

Novosibirsk State Technical University, 20, Karl Marx Ave., Novosibirsk, 630073, Russia

E-mail: Alblances@yandex.ru

Abstract. Ore-smelting furnaces are the biggest and the most powerful furnaces in which the electric arc is used for converting electric energy into heat. Studying electromagnetic field in their structural components is one of instruments in energy saving developments. Since an ore-smelting furnace is a complex electrical device, we are forced to make assumptions, which would allow reducing the complex problem to a set of more simple analytical or numerical problems admitting not only quantitative but also qualitative solutions with acceptable accuracy. There is an approach when an electromagnetic problem is reduced to calculating an equivalent circuit that comprises both resistances and reactances. For calculating electromagnetic fields, cascade equivalent circuits are well-known in electro-mechanics. Particularly, cascade equivalent circuits of magneto-electric induction heating systems may be used as prototypes for qualitative calculating electromagnetic field and eddy currents in the mantle of the ore-smelting furnace. In the paper, qualitative calculating the resistance losses in the mantle of the ore-smelting furnace with such cascade equivalent circuit is offered.

1. Introduction

Ore-smelting furnaces are the biggest furnaces in which the electric arc is used for converting electric energy into heat. In addition, ore-smelting furnaces are the most powerful among all the electrical devices. Therefore energy saving has primary importance when it is necessary to develop ore-smelting furnaces; and studying electromagnetic field in their structural components becomes one of instruments in such development.

In view of the fact that an ore-smelting furnace is a complex electrical device, studying electromagnetic field is difficult both in furnace interiors and in furnace exteriors. This significant circumstance forces us to make assumptions, which would allow reducing the complex problem to a set of more simple analytical or numerical problems admitting not only quantitative but also qualitative solutions with acceptable accuracy.

As an alternative of numerical methods, there is an approach when an electromagnetic problem is reduced to calculating an equivalent circuit that comprises both resistances and reactances. An extensive branch (known as partial equation equivalent circuits) has been actively worked out recently [1-3].

For calculating electromagnetic fields, cascade equivalent circuits on basis of Cartesian and cylindrical laminated models are well-known in electro-mechanics [4-10]. These circuits differ from that which are described in [1-3] since constants of cascade equivalent circuits result from reducing general solutions of partial differential equations to equations of a standard four-terminal network.

Particularly, cascade equivalent circuits are described in [10] for calculating eddy fields of magneto-electric induction heating systems that may be considered as unconventional electrical machines.

Calculating resistance losses in the mantle of the ore-smelting furnace may be carried out with a similar cascade equivalent circuit. If a furnace bath is round, then a mantle is cylindrical on a top and conical on a bottom. Therefore, in a strict sense, a problem should be solved as 3D. However if a conical bottom is neglected and a source is considered as the symmetrical three-phase current system, electromagnetic field becomes planar and resistance losses may be qualitatively calculated with the cascade equivalent circuit.

It is qualitative calculating resistance losses in the mantle of the ore-smelting furnace that are offered in this paper. The calculation is carried out with the cascade equivalent circuit that is analogous to the cascade equivalent circuit of the magneto-electric induction heating system.

2. The laminated model

The experimental data given in [11] show that the configuration of electrodes has not the considerable influence on electromagnetic losses within the furnace mantle. It allows using the approach given in [12] in respect to three-phase cable lines with conducting shells. This approach consists in the replacement of current-carrying conductors by equivalent current sheets.

Figure 1 shows the laminated model of the ore-smelting furnace. Arc-like current sheets that are located at the pitch circle diameter replace electrodes. Thus, the space within the furnace is divided into three layers marked as 1, 2 and 3.

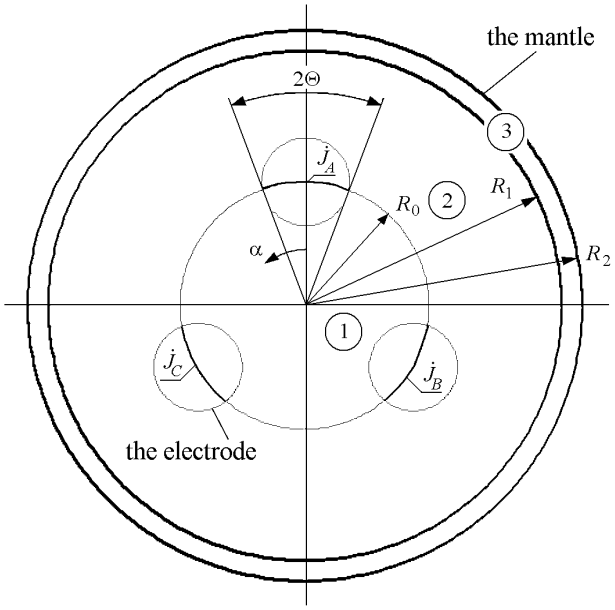

Figure 1. The laminated model of the ore-smelting furnace.

Let us synthesize the cascade equivalent circuit in which the certain four-terminal network would correspond to the each layer. In this equivalent circuit, a vector potential will be regarded as a voltage, and a tangential component of a magnetic intensity vector multiplied by a variable radius will be regarded as a current.

3. The three-phase system of current sheets as the source of traveling electromagnetic field

Prior to synthesizing the cascade equivalent circuit, let us consider the source of traveling electromagnetic field. The current sheet corresponds to the each electrode and the total electrode current is concentrated at the current sheet:

$$J_{\text{ph}} = \frac{I_{\text{ph}}}{\Theta d_{\text{p}}} = \frac{I_{\text{ph}}}{2\Theta R_0}, \tag{1}$$

where I_{ph} is the electrode current; $d_{\text{p}} = 2R_0$ is the pitch circle diameter; and 2Θ is the angle at which we can see the current sheet (from the mantle centre).

Within the accuracy that is acceptable for practical calculating, the angle Θ are determined as:

$$\Theta = \frac{d_{\text{el}}}{d_{\text{p}}}, \tag{2}$$

where d_{el} is the electrode diameter.

A curve of the current sheet at the pitch circle diameter (the phase *A*) is shown in Figure 2. If to expand this curve into Fourier's series then we will obtain:

$$J_A(\alpha) = \frac{I_{\text{ph}}}{2\pi R_0} + \frac{I_{\text{ph}}}{\pi\Theta R_0}\sum_k \frac{\sin k\Theta}{k}\cos k\alpha\,. \tag{3}$$

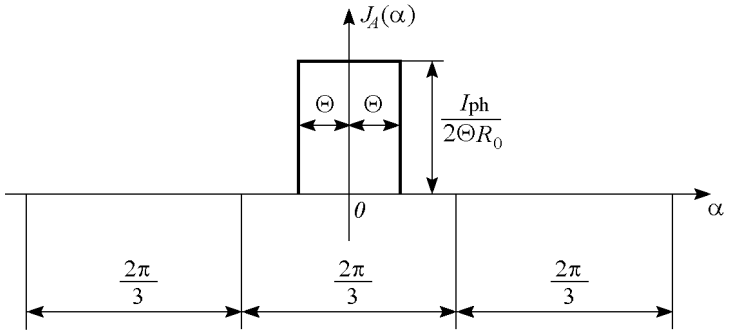

Figure 2. A curve of the current sheet at the pitch circle diameter (the phase *A*).

By analogy, for the phase *B* and the phase *C* we will obtain:

$$J_B(\alpha) = \frac{I_{\text{ph}}}{2\pi R_0} + \frac{I_{\text{ph}}}{\pi\Theta R_0}\sum_k \frac{\sin k\Theta}{k}\cos\left(k\alpha - \frac{2\pi}{3}\right), \tag{4}$$

$$J_C(\alpha) = \frac{I_{\text{ph}}}{2\pi R_0} + \frac{I_{\text{ph}}}{\pi\Theta R_0}\sum_k \frac{\sin k\Theta}{k}\cos\left(k\alpha + \frac{2\pi}{3}\right). \tag{5}$$

Expressions (3)-(5) are amplitudes of sinusoidal temporal functions:

$$J_A(\alpha,t) = \left(\frac{I_{\text{ph}}}{2\pi R_0} + \frac{I_{\text{ph}}}{\pi\Theta R_0}\sum_k \frac{\sin k\Theta}{k}\cos k\alpha\right)\sin\omega t\,, \tag{6}$$

$$J_B(\alpha,t) = \left(\frac{I_{\text{ph}}}{2\pi R_0} + \frac{I_{\text{ph}}}{\pi\Theta R_0}\sum_k \frac{\sin k\Theta}{k}\cos\left(k\alpha - \frac{2\pi}{3}\right)\right)\sin\left(\omega t - \frac{2\pi}{3}\right), \tag{7}$$

$$J_C(\alpha,t) = \left(\frac{I_{\text{ph}}}{2\pi R_0} + \frac{I_{\text{ph}}}{\pi\Theta R_0}\sum_k \frac{\sin k\Theta}{k}\cos\left(k\alpha + \frac{2\pi}{3}\right)\right)\sin\left(\omega t + \frac{2\pi}{3}\right), \tag{8}$$

where ω is the current angular frequency.

In the complex plane, these expressions (for the *k*-th harmonic) take the form:

$$\dot{J}_{Ak} = \frac{I_{\text{ph}}}{2\pi R_0} + \frac{I_{\text{ph}}}{\pi\Theta R_0}\frac{\sin k\Theta}{k}\cos k\alpha\,, \tag{9}$$

$$\dot{J}_{Bk} = \left(\frac{I_{\text{ph}}}{2\pi R_0} + \frac{I_{\text{ph}}}{\pi\Theta R_0}\frac{\sin k\Theta}{k}\cos\left(k\alpha - \frac{2\pi}{3}\right)\right)\mathrm{e}^{-j\frac{2\pi}{3}}, \tag{10}$$

$$\dot{J}_{Ck} = \left(\frac{I_{\text{ph}}}{2\pi R_0} + \frac{I_{\text{ph}}}{\pi \Theta R_0} \frac{\sin k\Theta}{k} \cos\left(k\alpha + \frac{2\pi}{3} \right) \right) \mathrm{e}^{j\frac{2\pi}{3}}. \tag{11}$$

Let us sum up these complex harmonics of the current sheets (9)-(11):

$$\dot{J}_k = \frac{I_{\text{ph}}}{\pi \Theta R_0} \frac{\sin k\Theta}{k} \left(\cos k\alpha \left(1 - \cos \frac{2k\pi}{3} \right) - j\sqrt{3} \sin k\alpha \cdot \sin \frac{2k\pi}{3} \right), \tag{12}$$

and all the harmonics in which the parameter k is multiple of 3 (and $k = 0$ too) will vanish, but if $k = 1, 4, 7, \ldots$ then the expression (12) will take the form:

$$\dot{J}_k = 1.5 \frac{I_{\text{ph}}}{\pi \Theta R_0} \frac{\sin k\Theta}{k} \mathrm{e}^{-jk\alpha}, \tag{13}$$

and if $k = 2, 5, 8, \ldots$ then the expression (12) will take the form:

$$\dot{J}_k = 1.5 \frac{I_{\text{ph}}}{\pi \Theta R_0} \frac{\sin k\Theta}{k} \mathrm{e}^{jk\alpha}. \tag{14}$$

Traveling waves (that are sources inducing eddy currents within the mantle) correspond to expressions (13) and (14):

$$J_k(\alpha, t) = 1.5 \frac{I_{\text{ph}}}{\pi \Theta R_0} \frac{\sin k\Theta}{k} \sin\left(k\omega t \pm k\alpha \right). \tag{15}$$

4. The cascade equivalent *A-H*-circuit of the system named "the mantle and electrode"

The cascade equivalent *A-H*-circuit of the system named "the mantle and electrodes" is shown in Figure 3. In this circuit, a vector potential is regarded as a voltage, and a tangential component of a magnetic intensity vector multiplied by a variable radius is regarded as a current.

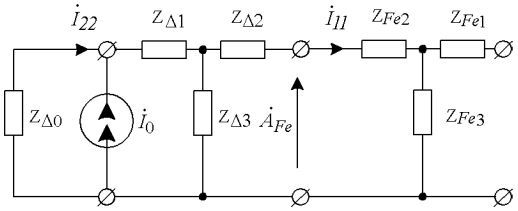

Figure 3. The cascade equivalent *A-H*-circuit of the system named "the mantle and electrodes".

In essence, this cascade equivalent *A-H*-circuit differs from the cascade equivalent *A-H*-circuit of the magneto-electric induction heating system described in [10] in the field source that is the magnitude of the function (13) multiplied by the pitch circle radius:

$$\dot{I}_0 = 1.5 \frac{I_{\text{ph}}}{\pi \Theta} \frac{\sin k\Theta}{k}. \tag{16}$$

In the equivalent *A-H*-circuit, there are three four-terminal cells. The middle cell corresponds to the layer marked as 2 (see Figure 1). Constants of this cell are given in [10]:

$$Z_{\Delta 1} = Z_{\Delta 2} = \frac{\mu_0}{k} \frac{\left(\frac{r_1}{r_0} \right)^k + \left(\frac{r_0}{r_1} \right)^k - 2}{\left(\frac{r_1}{r_0} \right)^k - \left(\frac{r_0}{r_1} \right)^k}, \tag{17}$$

$$Z_{\Delta 3} = \frac{\mu_0}{k} \frac{2}{\left(\frac{r_1}{r_0} \right)^k - \left(\frac{r_0}{r_1} \right)^k}. \tag{18}$$

If in expressions (17) and (18), the lesser radius tends to zero then constants of the left cell (corresponding to the layer marked as 1 in Figure 1) may be obtained. The transversal resistance will vanish and the single longitudinal resistance will determined as:

$$Z_{\Delta 0} = \frac{\mu_0}{k}. \tag{19}$$

The right cell corresponds to the furnace mantle i.e. the layer marked as 3 (see Figure 1). In this cell, output terminals are open since electromagnetic field is absent beyond the penetration depth. Constants of this cell are also given in [10] and determined by Hankel functions of the first and second kind that cannot be calculated if the argument is too large. In this case, certain asymptotic approximations are usually used [13]. On other hand, an alternative approach may be advised.

In the *Mathcad* 11, there are scaled Hankel functions. For example, first- and second-order scaled Hankel functions are determined by Hankel functions as:

$$\mathrm{H}_1^{\mathrm{sc}(1)}(z) = \mathrm{H}_1^{(1)}(z)\mathrm{e}^{-jz}, \tag{20}$$

$$\mathrm{H}_1^{\mathrm{sc}(2)}(z) = \mathrm{H}_1^{(2)}(z)\mathrm{e}^{jz}, \tag{21}$$

$$\mathrm{H}_2^{\mathrm{sc}(1)}(z) = \mathrm{H}_2^{(1)}(z)\mathrm{e}^{-jz}, \tag{22}$$

$$\mathrm{H}_2^{\mathrm{sc}(2)}(z) = \mathrm{H}_2^{(2)}(z)\mathrm{e}^{jz}. \tag{23}$$

Replacing Hankel functions by scaled Hankel functions in formulas given in [10], we can obtain constants of the cell corresponding to the layer marked as 3 (see Fig. 1) in the form:

$$\begin{aligned} Z_{Fe2} = {} & \frac{\mu}{\nu_k r_1}\left\{\frac{\mathrm{H}_k^{\mathrm{sc}(1)'}(\nu_k r_2)\mathrm{H}_k^{\mathrm{sc}(2)'}(\nu_k r_1)}{\mathrm{e}^{j\nu_k(r_1-r_2)}} - \frac{\mathrm{H}_k^{\mathrm{sc}(1)'}(\nu_k r_1)\mathrm{H}_k^{\mathrm{sc}(2)'}(\nu_k r_2)}{\mathrm{e}^{-j\nu_k(r_1-r_2)}}\right\}^{-1} \times \\ & \times\left\{\mathrm{H}_k^{\mathrm{sc}(1)'}(\nu_k r_2)\left[\mathrm{H}_k^{\mathrm{sc}(2)}(\nu_k r_2) - \mathrm{H}_k^{\mathrm{sc}(2)}(\nu_k r_1)\mathrm{e}^{-j\nu_k(r_1-r_2)}\right] - \right. \\ & \left. - \mathrm{H}_k^{\mathrm{sc}(2)'}(\nu_k r_2)\left[\mathrm{H}_k^{\mathrm{M}(1)}(\nu_k r_2) - \mathrm{H}_k^{\mathrm{sc}(1)}(\nu_k r_1)\mathrm{e}^{j\nu_k(r_1-r_2)}\right]\right\}, \end{aligned} \tag{24}$$

$$\begin{aligned} Z_{Fe3} = {} & \frac{\mu}{\nu_k r_2}\left\{\frac{\mathrm{H}_k^{\mathrm{sc}(1)'}(\nu_k r_2)\mathrm{H}_k^{\mathrm{sc}(2)'}(\nu_k r_1)}{\mathrm{e}^{j\nu_k(r_1-r_2)}} - \frac{\mathrm{H}_k^{\mathrm{sc}(1)'}(\nu_k r_1)\mathrm{H}_k^{\mathrm{sc}(2)'}(\nu_k r_2)}{\mathrm{e}^{-j\nu_k(r_1-r_2)}}\right\}^{-1} \times \\ & \times\left[\mathrm{H}_k^{\mathrm{sc}(2)'}(\nu_k r_1)\mathrm{H}_k^{\mathrm{sc}(1)}(\nu_k r_1) - \mathrm{H}_k^{\mathrm{sc}(1)'}(\nu_k r_1)\mathrm{H}_k^{\mathrm{sc}(2)}(\nu_k r_1)\right], \end{aligned} \tag{25}$$

where $\nu_k = \sqrt{-j\omega k\mu\gamma}$; γ is the mantle conductivity; μ is the mantle magnetic permeability.

The first-order derivatives of scaled Hankel functions are calculated as:

$$\mathrm{H}_k^{\mathrm{sc}(1)'}(\nu_k r) = \frac{k\,\mathrm{H}_k^{\mathrm{sc}(1)}(\nu_k r) - \nu_k r\,\mathrm{H}_{k+1}^{\mathrm{sc}(1)}(\nu_k r)}{\nu_k r}, \tag{26}$$

$$\mathrm{H}_k^{\mathrm{sc}(2)'}(\nu_k r) = \frac{k\,\mathrm{H}_k^{\mathrm{sc}(2)}(\nu_k r) - \nu_k r\,\mathrm{H}_{k+1}^{\mathrm{sc}(2)}(\nu_k r)}{\nu_k r}. \tag{27}$$

After calculating vector potentials and tangent components of magnetic intensity vectors with the cascade equivalent *A*-*H*-circuit, resistance losses in the mantle are calculated on the basis of Poynting's theorem.

5. Test results

Geometrical data are given in Table 1. The mantle material is steel; the conductivity is

$4 \cdot 10^6$ Ohm^{-1}m^{-1}; the relative magnetic permeability is 100; the electrode conductivity (for numerical calculating) is $1.7 \cdot 10^5$ Ohm^{-1}m^{-1}; the electrode current is 93 kA; the current frequency is 50 Hz.

Table 1. Geometrical data of the system named "the mantle and electrodes"

Bath diameter, mm	8800
Wall depth, mm	25
Pitch circle diameter, mm	3950
Electrode diameter, mm	1400

Calculation of the resistance losses in the mantle is given in Table 2. The good correlation is evident between analytical and numerical results.

Table 2. Resistance losses in the mantle (kW per the unit bath height)

Calculating with the cascade equivalent circuit	First harmonic	35.821
	Second harmonic	8.782
	Fourth harmonic	0.284
	Total	44.887
Numerical calculating (*FEMM* 4.2)	–	41.853

Nevertheless, the offered 2D model is only approximate. Only qualitative calculating is possible here. The conical mantle bottom, the source asymmetry and the low ratio of the mantle height to the mantle diameter don't allow considering electromagnetic field as planar in a strict sense. Therefore, quantitative calculating is possible only in the 3D model.

6. Conclusion

For modeling eddy electromagnetic field and calculating resistance losses in the mantle of the ore-smelting furnace, the cascade equivalent *A*-*H*-circuit is offered.

Electromagnetic field is considered as planar; therefore only qualitative calculating is possible in this cascade equivalent *A*-*H*-circuit. In this model, the field sources are equivalent current sheets replacing current-carrying electrodes. These current sheets are located at the pitch circle diameter.

The good correlation is evident between analytical and numerical results. Nevertheless, the offered 2D model is approximate and quantitative calculating is possible only in the 3D model.

References

[1] Voloboev V P, Klimenko V P 2013 The finite element method and the graph theory *Mathematical Machines and Systems* **4** 114–125 (in Russian)
[2] Freschi F, Repetto M 2008 A General Framework for Mixed Structured / Unstructured PEEC Modeling *ACES J.* **23** 200–206
[3] Alotto P, Desideri F, Freschi F, Maschio A and Repetto M 2011 Dual-PEEC modeling of a two-port TEM cell for VHF applications *IEEE Trans. Magn.* **47** 1486–1489
[4] Freeman E M 1968 Travelling waves in induction machines: input impedance and equivalent circuits *IEE Proc.* **115(12)** 1772–1776
[5] Freeman E M 1974 Equivalent circuits from electromagnetic theory low-frequency induction devices *IEE Proc.* **121(10)** 1117–1121
[6] Freeman E M, Bland T G 1976 Equivalent circuit of concentric cylindrical conductors in an axial alternating magnetic field *IEE Proc.* **123(2)** 149–152
[7] Inkin A I 1975 The circuit approximation of linear mediums influenced by electromagnetic field

Electricity **4** 64–67 (in Russian)
[8] Inkin A I 2002 *Electromagnetic fields and parameters of electric machines: tutorial* (Novosibirsk: UKEA) p 464 (in Russian)
[9] Litvinov B V, Davidenko O B 2008 *Standard cells and cascade equivalent circuits of electric machines: monograph* (Novosibirsk: NSTU) p 215 (in Russian)
[10] Inkin A I, Aliferov A I Blanc A V 2013 *Electrothermal calculations of electroheating installations based on universal cascade equivalent circuits: monograph* (Novosibirsk: NSTU) p 202 (in Russian)
[11] Bikeev R A 2004 *Dynamic conditions in electro-mechanical systems of arc steel-smelting furnaces and their influence upon the input active power: candidate's dissertation* (Novosibirsk: NSTU) p 229 (in Russian)
[12] Inkin A I, Reicherdt A A 1999 The mathematical model for calculating electromagnetic processes in three-phase cables with the conducting shell *Electricity* **5** 28–34 (in Russian)
[13] Angot A 1967 *Complements de mathématiques a l'usage des ingénieurs de l'elektrotechnique et des télécommunications*: translation from French into Russian under the editorship of K.S. Shifrin (Moscow: Science) p 780 (in Russian)